Energy Materials

Supplementary Materials

Modulating electronic structure of Co-N_5S_1 sites in Co single atom catalysts via phosphorus incorporation and nanoclusters to promote oxygen electrocatalytic activity

Jing Peng[1], Ting Xue[1], Zhitong Li[1], Junwei Shi[1], Xingzhu Wang[1,2,*], Baomin Xu[1,*]

[1]Department of Materials Science and Engineering, and SUSTech Energy Institute for Carbon Neutrality, Southern University of Science and Technology, Shenzhen 518055, Guangdong, China.
[2]Shenzhen Putai Technology Co., Ltd, Shenzhen 518110, Guangdong, China.

[*]**Correspondence to:** Prof. Xingzhu Wang, Department of Materials Science and Engineering, and SUSTech Energy Institute for Carbon Neutrality, Southern University of Science and Technology, Taoyuan Street, Nanshan district, Shenzhen 518055, Guangdong, China. Shenzhen Putai Technology Co., Ltd, Guanlan Street, Longhua District, Shenzhen 518110, Guangdong, China. E-mail: wangxz@sustech.edu.cn; Prof. Baomin Xu, Department of Materials Science and Engineering, and SUSTech Energy Institute for Carbon Neutrality, Southern University of Science and Technology, Taoyuan Street, Nanshan District, Shenzhen, 518055, China. E-mail: xubm@sustech.edu.cn

In the Supplementary Materials, the SEM pictures, XRD patterns, and N_2 isothermal adsorption/desorption curves, LSV curves at different rotation rates, K-L plots, CV curves, EIS spectrums, the theoretic ORR pathway for Co_{SA+NC}/SC and Co_{SA+NC}/NSC have been presented in detail.

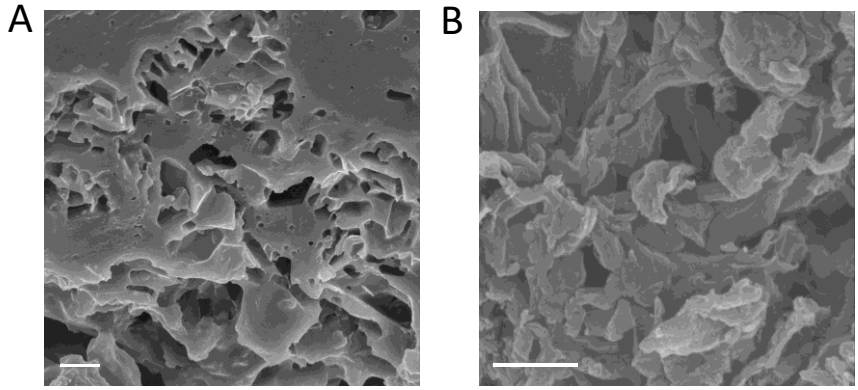

Supplementary Figure 1. SEM pictures of (A) Co_{SA+NC}/SC and (B) Co_{SA+NC}/NSC.

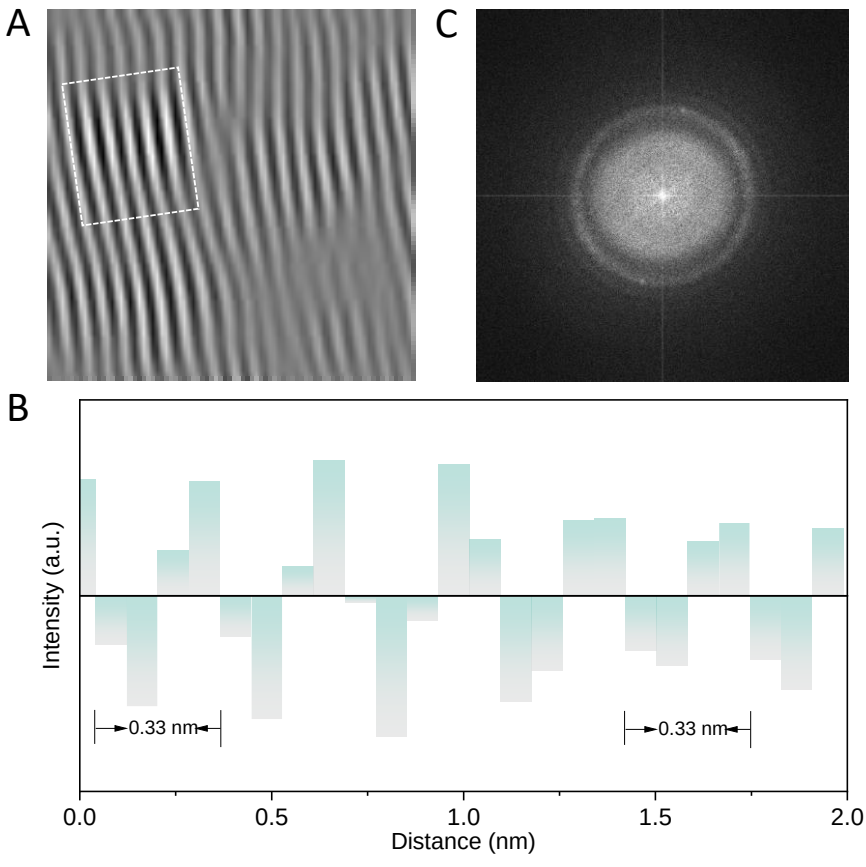

Supplementary Figure 2. (A) the enlarged lattice fringes refer to the circled area in Figure 1E. (B) the lattice spacing corresponding to the circled area in Figure S2A. (C) The selective electron diffraction pattern in Co_{SA+NC}/NPSC.

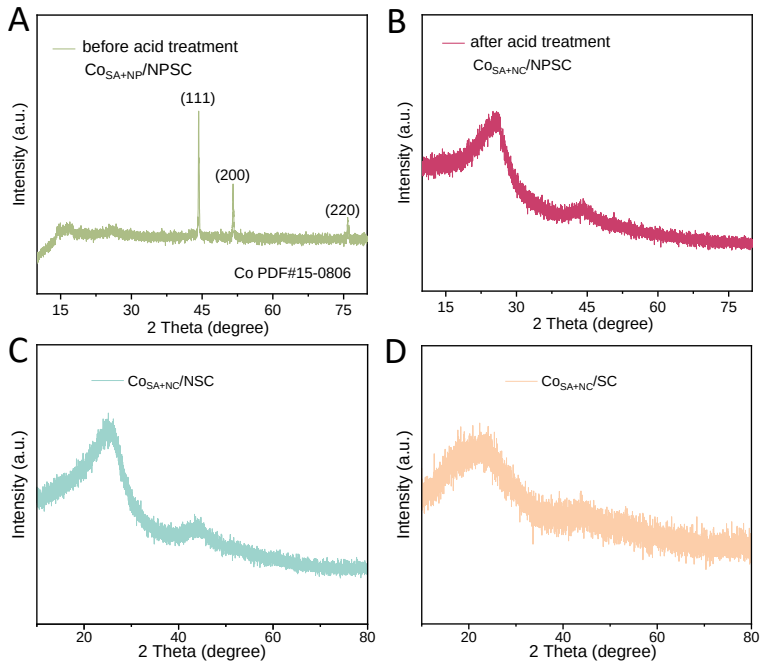

Supplementary Figure 3. XRD patterns of (A) Co_{SA+NP}/NPSC, (B) Co_{SA+NC}/NPSC, (C) Co_{SA+NC}/NSC and (D) Co_{SA+NC}/SC.

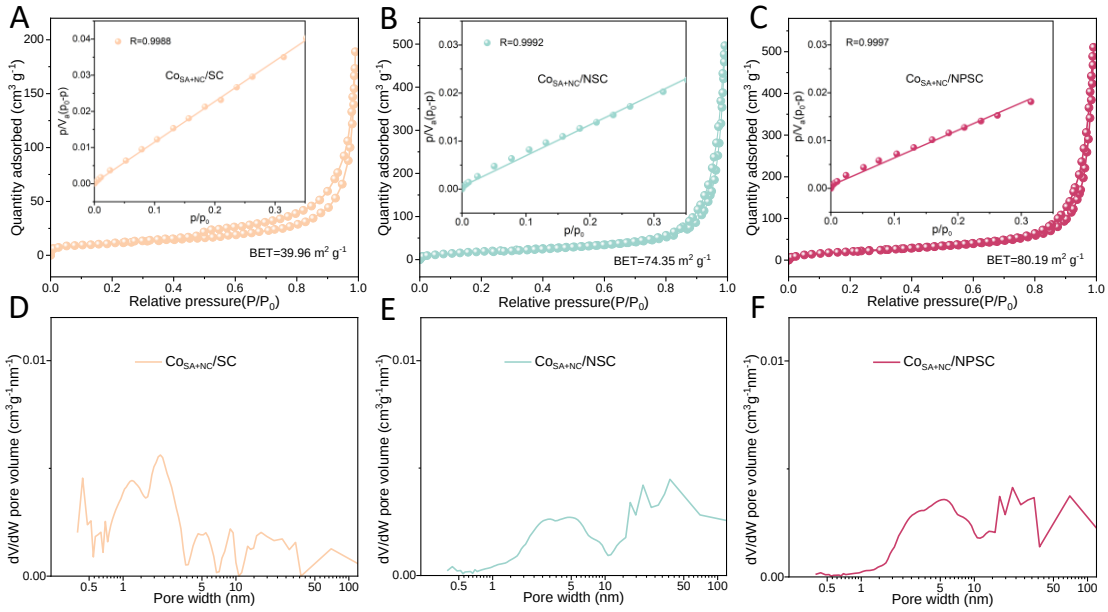

Supplementary Figure 4. N_2 isothermal adsorption/desorption curves and multi-point BET fitting curves of (A) Co_{SA+NC}/SC, (B) Co_{SA+NC}/NSC, and (C) Co_{SA+NC}/NPSC. The aperture distribution of (D) Co_{SA+NC}/SC, (E) Co_{SA+NC}/NSC, and (F) Co_{SA+NC}/NPSC.

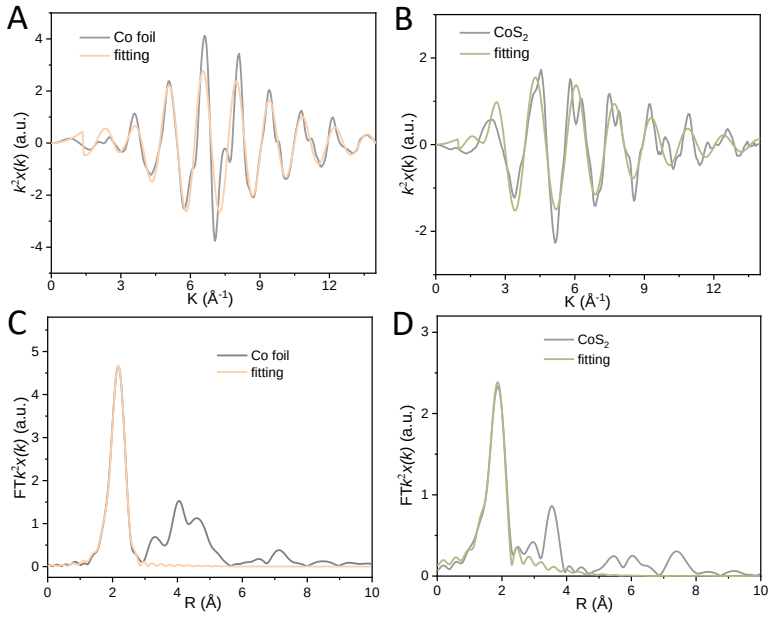

Supplementary Figure 5. EXAFS k space fitting curves of Co k-edge in (A) Co foil and (B) CoS_2. Experimental and the fitting FT-EXAFS curves at the Co K-edge of (C) Co foil and (D) CoS_2.

Oxygen reduction reaction (ORR) polarization curves were recorded in O_2-saturated 0.1 M KOH within the potential range of 1.2 to 0.2 V, at room temperature and a rotation rate of 1600 rpm. By integrating the ORR polarization curves across various rotation rates (400-2025 rpm) and applying the Koutecky-Levich (K-L) equations (1-3), the electron transfer number (n) during the ORR process was determined:

$$\frac{1}{J} = \frac{1}{J_L} + \frac{1}{J_K} = \frac{1}{B\omega^{0.5}} + \frac{1}{J_K} \quad (1)$$

$$B = 0.62nFC_0(D_0)^{\frac{2}{3}}v^{-\frac{1}{6}} \quad (2)$$

$$J_K = nFkC_0 \quad (3)$$

where J represented the measured current density, and B was derived from the Levich equation using the slope of the K-L plot. The terms J_K and J_L denoted the kinetic and diffusion-limited current densities, respectively. The current densities that restrict diffusion and kinetics were denoted by J_K and J_L, respectively. In the equations, n was the number of electrons transferred, F meant the Faraday constant (96485 C mol^{-1}), C_0 signified the bulk O_2 concentration (1.26×10^{-6} mol cm^{-3}), D_0 was designated as the diffusion coefficient of O_2 in 0.1 M KOH (1.93×10^{-5} cm^2 s^{-1}), and v symbolized the

kinematic viscosity of the electrolyte (0.01 $cm^2 s^{-1}$). In addition, potential-hold tests at 0.7 V were conducted to further evaluate the catalyst's stability. Prior to oxygen evolution reaction (OER) activity testing, any bubbles on the catalyst surface were removed, and the working electrode was activated. Polarization curves were obtained at a scan rate of 5 mV s^{-1} between 1.1 and 1.8 V (vs. RHE). The durability of the catalysts was further examined via continuous chronoamperometric testing over a 24 h period. The Tafel slope for the ORR/OER processes was calculated using the following equation:

$$\eta = a + b\log(j) \quad (4)$$

where j was designated as the current density, a symbolized the Tafel constant, b was denoted as the Tafel slope, and η represented the overpotential at a given current density.

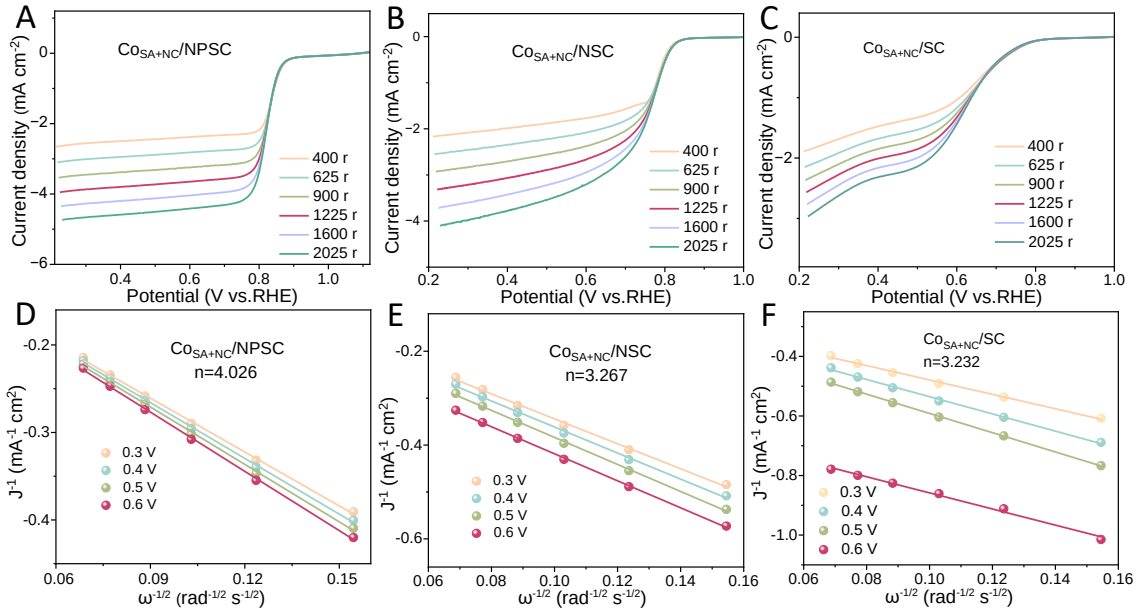

Supplementary Figure 6. LSV curves at different rotation rates in rpm of (A) Co_{SA+NC}/NPSC, (B) Co_{SA+NC}/NSC and (C) Co_{SA+NC}/SC. (D-E) K-L plots of Co_{SA+NC}/NPSC, Co_{SA+NC}/NSC and Co_{SA+NC}/SC, respectively.

The electrochemically active surface area (ECSA) was further estimated to reveal the number of exposed active sites and the effective active surface area of the catalyst during the ORR/OER processes. The double-layer capacitance (C_{dl}) was used as an indicator to quantitatively determine the ECSA, calculated from the following

equations:

$$C_{dl} = v \times ECSA \quad (5)$$

$$C_{dl} = \frac{I_c}{v} \quad (6)$$

where ν meant the scan rate (mV s^{-1}), and I_c was designated as the charging current (mA).

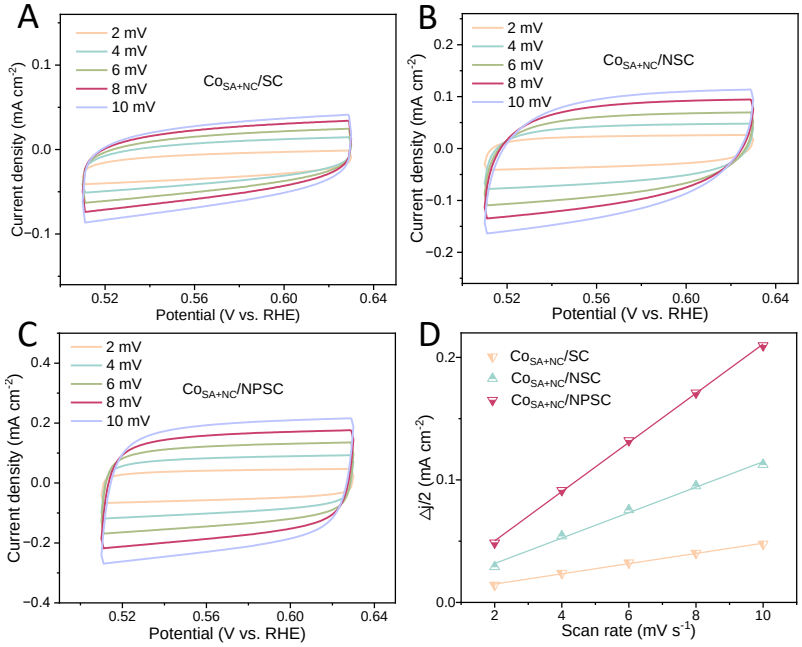

Supplementary Figure 7. CV curves for (A) Co_{SA+NC}/SC, (B) Co_{SA+NC}/NSC and (C) Co_{SA+NC}/NPSC at the overpotential window of 0.51-0.64 V. (D) The calculated C_{dl} values.

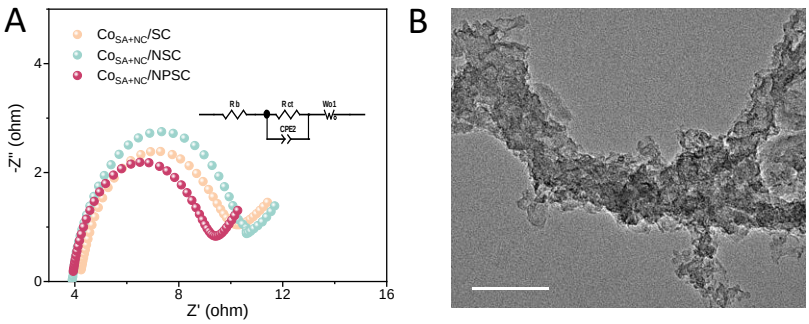

Supplementary Figure 8. (A) EIS spectrums of freshed flexbile ZABs at 0 ℃, (B) the TEM picture of Co_{SA+NC}/NPSC after cycling for several hours in Co_{SA+NC}/NPSC based flexible ZAB.

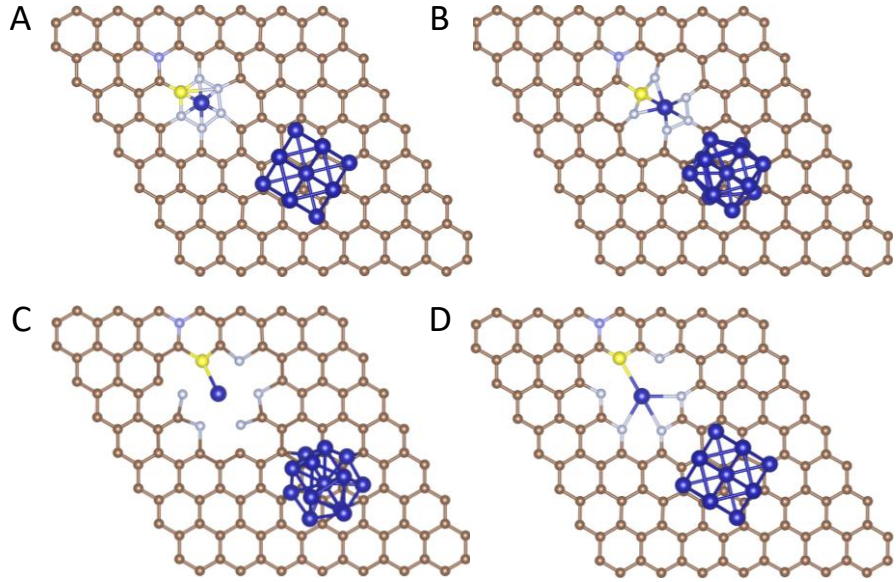

Supplementary Figure 9. Possible CoN_5S_1 and nanocluster structures in Co_{SA+NC}@NPSC.

As shown in Figure S9, we constructed possible models with different CoN_5S_1 arrangements of Co single atoms. According to the criteria of minimal formation energy and a stable oxygen intermediate structure, the optimized model was chosen as the energetically most favorable configuration and adopted for DFT studies.

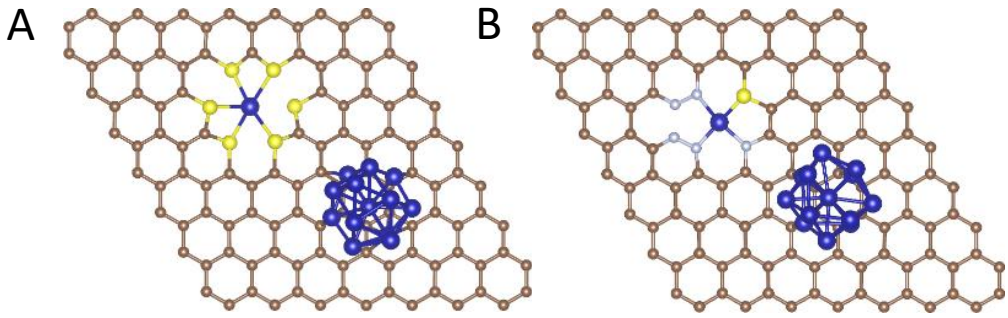

Supplementary Figure 10. Schematic presentation of atomic model for (A) Co_{SA+NC}/SC and (B) Co_{SA+NC}/NSC.

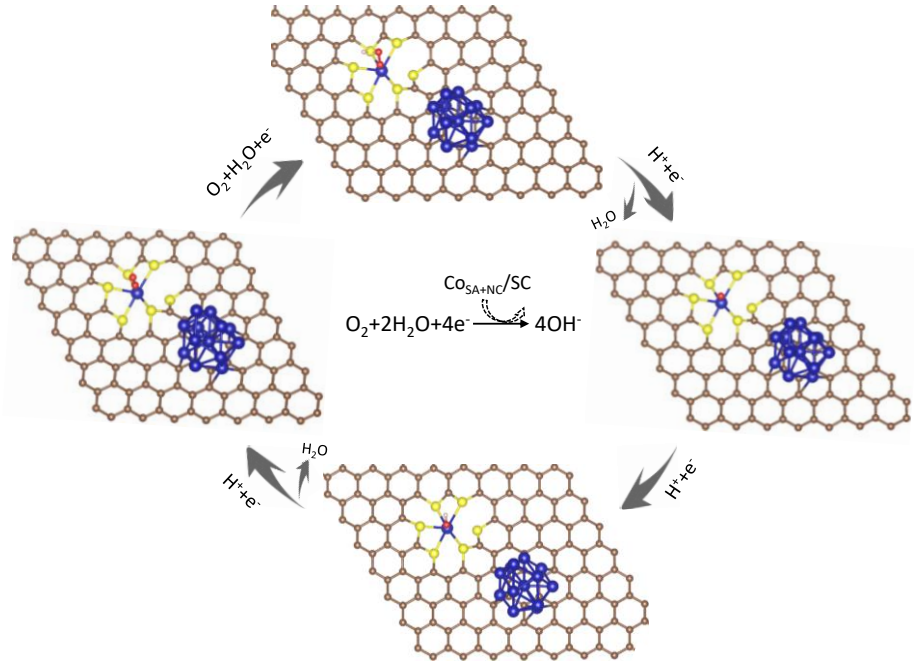

Supplementary Figure 11. Illustration of ORR process on CoS_6 sites based on Co_{SA+NC}/SC catalyst.

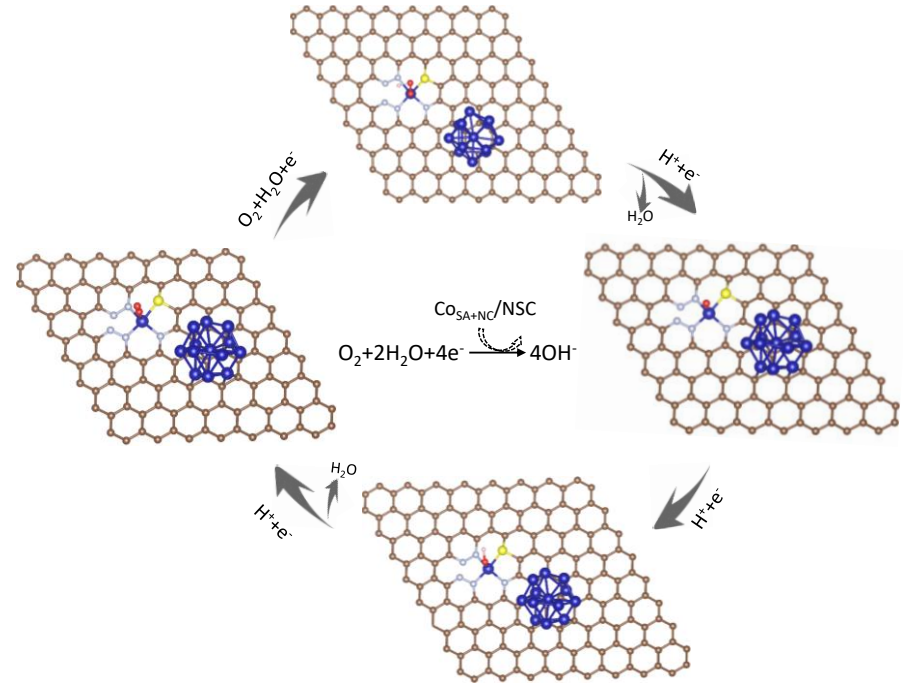

Supplementary Figure 12. Illustration of ORR process on CoN_5S_1 sites based on Co_{SA+NC}/NSC catalyst.

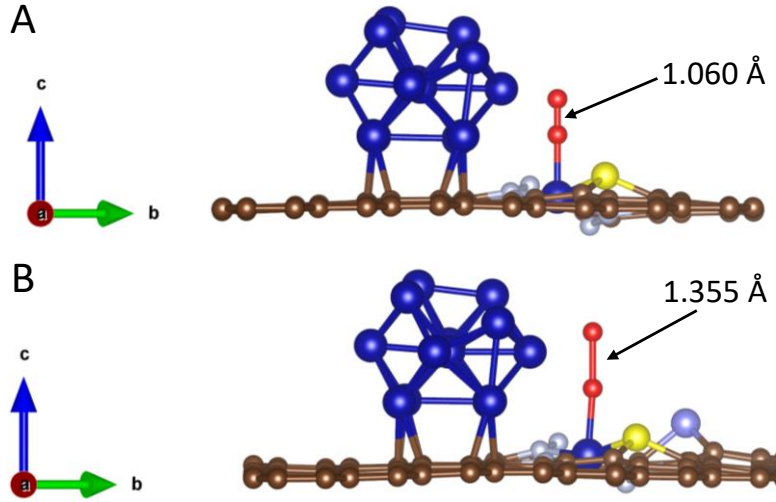

Supplementary Figure 13. O_2 adsorption models of (A) Co_{SA+NC}/NSC and (B) Co_{SA+NC}/NPSC, and the corresponding stretching degree of O-O bond.

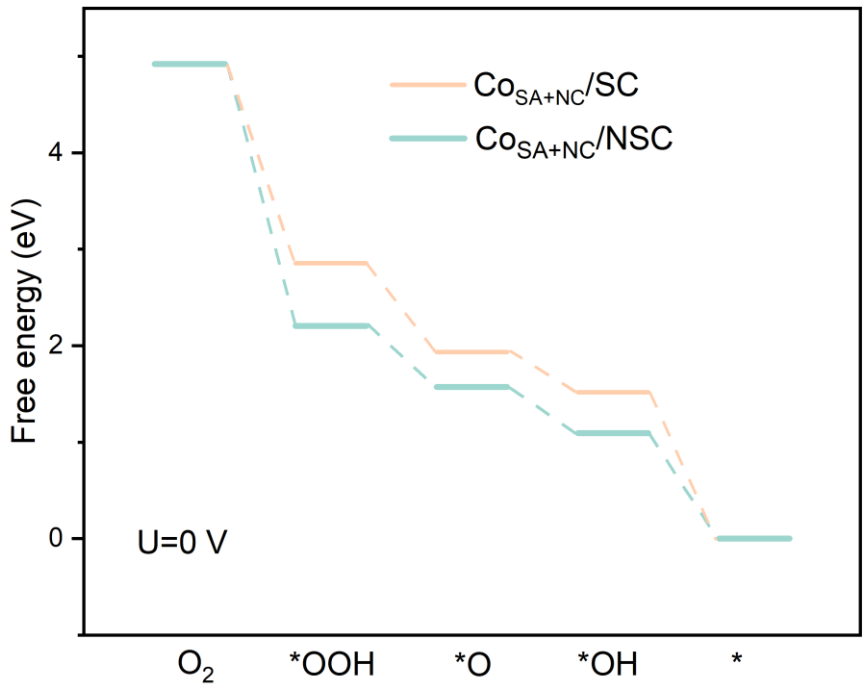

Supplementary Figure 14. Pathways for the Co_{SA+NC}/SC and Co_{SA+NC}/NSC at 0 V.

Table S1. ICP-AES analysis of Co atoms in Co_{SA+NP}/NPSC and Co_{SA+NC}/NPSC

Sample	Co (wt%)	P (wt%)	S (wt%)
Co_{SA+NP}/NPSC	28.87%	0.19%	1.06%
Co_{SA+NC}/NPSC	1.64%	/	/

Table S2. EXAFS fitting parameters at the Co K-edge for the catalyst and corresponding reference samples（S_0^2=0.76）

Sample	Shell	[a]*CN*	[b]*R* (Å)	[c]σ^2(Å^2)	[d]ΔE_0 (eV)	*R* factor
Co foil	Co-Co	12*	2.49±0.01	0.0064	7.0±0.7	0.0014
Co_{SA+NC}/NPSC	Co-N	5.3±0.3	2.03±0.01	0.0107	-2.7±1.6	0.0042
	Co-S	1.3±0.3	2.32±0.01	0.0045		
	Co-Co	5.1±0.5	2.46±0.01	0.0185		
CoS_2	Co-S	6.3±0.2	2.31±0.01	0.0055	3.7±0.9	0.0054

[a]*CN*, coordination number; [b]*R*, the distance to the neighboring atom; [c]σ^2, the Mean Square Relative Displacement (MSRD); [d]ΔE_0, inner potential correction; *R* factor indicates the goodness of the fit. S_0^2 was fixed to 0.76, according to the experimental EXAFS fit of Co foil by fixing *CN* as the known crystallographic value. * This value was fixed during EXAFS fitting, based on the known structure of Co. Fitting range: 3.0 ≤ *k* (/Å) ≤ 14.0 and 1.0 ≤ *R* (Å) ≤ 3.0 (Co foil); 3.0 ≤ *k* (/Å) ≤ 11.2 and 1.0 ≤ *R* (Å) ≤ 3.0 (sample); 3.0 ≤ *k* (/Å) ≤ 11.3 and 1.0 ≤ *R* (Å) ≤ 2.5 (CoS_2). A reasonable range of EXAFS fitting parameters: 0.700 < S_0^2 < 1.000; *CN* > 0; σ^2 > 0 Å^2; $|\Delta E_0|$ < 10 eV; *R* factor < 0.02.

XAFS measurements and analysis details

For Wavelet Transform analysis, the χ(*k*) exported from Athena was imported into the Hama Fortran code[1]. The parameters were listed as follow: *R*-range, 0.0 - 4.0 Å, *k*-range, 0 - 14.0 Å^{-1} for sample; *k* weight, 2; and Morlet function with κ=10, σ=1 was used as the mother wavelet to provide the overall distribution. Data reduction, data analysis, and EXAFS fitting were performed and analyzed with the Athena and Artemis programs of the Demeter data analysis packages[2] that utilizes the FEFF6 program[3] to fit the EXAFS data. The energy calibration of the sample was conducted through a standard Co foil, which as a reference was simultaneously measured. A linear function was subtracted from the pre-edge region, then the edge jump was normalized using Athena software. The χ(*k*) data were isolated by subtracting a smooth, third-order

polynomial approximating the absorption background of an isolated atom. The k^2-weighted $\chi(k)$ data were Fourier transformed after applying a Hanning window function (Δk =1.0). For EXAFS modeling, the global amplitude EXAFS (*CN, R,* σ^2 and ΔE_0) were obtained by nonlinear fitting, with least-squares refinement, of the EXAFS equation to the Fourier-transformed data in *R*-space, using Artemis software, EXAFS of the Co foil is fitted and the obtained amplitude reduction factor S_0^2 value (0.76) was set in the EXAFS analysis to determine the coordination numbers (*CNs*) in the Co-N, Co-S, Co-Co scattering path in sample.

REFERENCES

1. Funke H, Scheinost AC, and Chukalina M: Wavelet analysis of extended x-ray absorption fine structure data. *Physical Review B* 2005; 71: 094110. DOI:10.1103/PhysRevB.71.094110.

2. Ravela B and Newville Anon M: ATHENA, ARTEMIS, HEPHAESTUS: data analysis for X-ray absorption spectroscopy using IFEFFIT *J Synchrotron Rad* 2005; 12: 537-541. DOI: 10.1107/S0909049505012719.

3. Zabinsky SI, Rehr JJ and Ankudinov A Multiple-scattering calculations of X-ray-absorption spectra. *Phys Rev B* 1995; 52: 2995-3009. DOI:10.1103/PhysRevB.52.2995.